(10) F. Kanamaru, S. Yamanaka, M. Koizumi, and S. Nagai, *Chem. Lett.*, 373 (1974).
(11) R. M. Barrer, "Non-stoichiometric Compounds", L. Mandelcorn, Ed., Academic Press, New York, N.Y., 1964, p 309.
(12) H. Deuel, *Kolloid-Z.*, **124**, 164 (1951).
(13) A. Clearfield and G. D. Smith, *Inorg. Chem.*, **8**, 431 (1969).
(14) S. Yamanaka and M. Koizumi, *Clays Clay Miner.*, **23**, 477 (1975).
(15) A. Clearfield, R. H. Blessing, and J. A. Stynes, *J. Inorg. Nucl. Chem.*, **30**, 2249 (1968).
(16) A. Clearfield, A. L. Landis, A. S. Medina, and J. H. Troup, *J. Inorg. Nucl. Chem.*, **35**, 1099 (1973).
(17) A. Clearfield and J. A. Stynes, *J. Inorg. Nucl. Chem.*, **26**, 117 (1964).
(18) J. Kumamoto, J. R. Cox, Jr., and F. H. Westheimer, *J. Am. Chem. Soc.*, **78**, 4858 (1956).
(19) P. C. Haake and F. H. Westheimer, *J. Am. Chem. Soc.*, **83**, 1102 (1961).
(20) F. R. Atherton, H. T. Openshaw, and A. R Todd, *J. Chem. Soc.*, 382 (1945).
(21) A. K Nelson and A. D. F Toy, U.S. Patent 3 146 255 (1949).
(22) C. S. Hanes and F. A. Isherwood, *Nature (London)*, **164**, 1107 (1949).
(23) E. Karl-Kroupa, *Anal. Chem.*, **28**, 1091 (1956).
(24) P. G. Shewmon, "Diffusion in Solids", McGraw-Hill, New York, N.Y., 1963.
(25) "X-ray Powder Diffraction File", Joint Committee on Powder Diffraction Standards, Philadelphia, Pa.
(26) D. E. Corgridge, *Top. Phosphorus Chem.*, **6**, 235 (1969).
(27) E. D. Whitney, *Trans. Faraday Soc.*, **61**, 1991 (1965).
(28) A. Clearfield, *Inorg. Chem.*, **3**, 146 (1964).
(29) J. R. Van Wazer, "Phosphorus and its Compounds", Vol. 1, Interscience, New York, N.Y., 1958, pp 441, 459, and 581.
(30) G. Lagaly and A. Weiss, *Kolloid Z. Z. Polym.*, **248**, 968 (1971).
(31) D. M. C. MacEwan, A. R. Amil, and G. Brown, "The X-ray Identification and Crystal Structures of Clay Materials", G. Brown, Ed., Mineralogical Society, London, 1961, p 393.
(32) G. Lagaly and A. Weiss, *Angew. Chem., Int. Ed. Engl.*, **10**, 558 (1971).

Contribution from the Department of Chemistry,
Louisiana State University, Baton Rouge, Louisiana 70803

Absorption and Magnetic Circular Dichroism Spectra of Chromium(III) in Dicesium Sodium Yttrium Hexachloride

ROBERT W. SCHWARTZ

Received February 18, 1976 AIC60131I

The electron paramagnetic resonance, absorption, and magnetic circular dichroism spectra of Cr^{3+}:Cs_2NaYCl_6 have been measured, the latter two down to 6 K. Transitions to three doublets (^2E_g, $^2T_{1g}$, and $^2T_{2g}$) and all three quartets ($^4T_{2g}$, $^4T_{1g}$ (I and II)) were observed. The ground-state g value was 1.984 ± 0.001 and the optical spectra were fit with the parameters $F_2 = 1050$, $F_4 = 90$ ($B = 600$, $C = 3150$), $Dq = 1280$, and $\alpha = 78.2$, all in cm^{-1}. The value of ζ, the spin–orbit coupling constant, was found to vary with the electronic term. This is ascribed to varying degrees of covalency. At 6 K magnetic dipole allowed origins were observed for numerous transitions. A rich vibrational structure was also seen in many transitions at this temperature. This has been assigned effectively with the site group approximation considering only the $CrCl_6^{3-}$ moiety. A progression in an e_g vibrational mode was found in three terms but no evidence of any other Jahn–Teller effect was observed.

Introduction

As part of a continuing study of the electronic structure of metal ions at sites of undistorted O_h symmetry[1] the optical absorption, magnetic circular dichroism (MCD), and electron paramagnetic resonance (EPR) spectra of Cr^{3+}:Cs_2NaYCl_6 have been measured and are reported herein. The use of O_h symmetry simplifies theoretical considerations for d-electron systems as only one crystal field parameter, Dq, need be considered. In addition the full power of group theoretical calculations can be applied to the MCD with the least possible ambiguity. Experimentally this geometry has a simplifying effect as the fewest possible states are found; i.e., the maximum possible degeneracies still exist. The use of chloride as a ligand also aids in simplifying the observed spectrum as no strictly ligand vibrations are possible and only metal–ligand vibrations are observed. In addition this particular host lattice has the advantage that all observed transitions are well separated. Thus the problem of overlap which made any detailed interpretation of the spectrum of Cr^{3+}:K_2NaGaF_6[2] extremely difficult is eliminated.

MCD has recently been used with some success in interpreting the spectra of first-row transition metal ions.[3] In particular two studies have appeared concerning the spectrum of Cr^{3+} in octahedral (MgO[4]) and near-octahedral (potassium alum[5]) environments. The latter paper presents many general theoretical results and significant use has been made of these in the present study. A number of studies have appeared on the EPR[6] and optical spectra[7] of Cr^{3+} in octahedral or near-octahedral environments. At least one study[8] gave a detailed interpretation of the vibronic structure observed in the $^2E_g \rightarrow {}^4A_{2g}$ phosphorescence of $Cr(NH_3)_6^{3+}$. In this case the $\nu_2(e_g)$ vibration was found to be an important progression-forming mode. This also seems to be the case in the present study. The isoelectronic divalent vanadium ion has also been studied as the octahedral VF_6^{4-} species.[9] In this species a large reduction in the splitting between spin–orbit components of the lowest vibronic level of the $^4T_{2g}$ term was found. This manifestation of the Ham effect[10] might also be observed in the present case but (see below) the results are not as clearly defined.

Experimental Section

Most spectra were recorded at the University of Virginia using equipment and technique previously described.[1a,b] Spectral slit widths (shown on each spectrum) were narrow enough to eliminate any machine broadening. The samples used were checked for depolarization and strain (zero-field CD) and neither of these proved to be a problem. Temperature dependence of the MCD showed the spectrum to be composed mostly of c_0 terms.[11] In the spin-forbidden transitions (the expected sign) a_1 terms were in many cases resolved upon heating. Some temperature- and field-dependence data for the spin-allowed transitions were recorded using an Oxford Instruments Spectro-Mag II system and a Jasco J20 spectrometer which has had an absorption mode added. Absolute temperatures on this latter system should be good to ±0.3 K with temperature differences good to ±0.1 K. Cs_2NaYCl_6 was prepared by method E of Morss, et al.[12] Crystals were grown as previously described.[1a,b] Cr^{3+} was added as $Cs_2NaCrCl_6$ prepared in the same way. As the actual Cr^{3+} concentration of the samples was not known, all MCD and absorption values are in arbitrary units. However as the quantity of most interest, MCD/D, is independent of concentration, this proves to be no problem. These ratios should be good to ±20% except on the weakest transitions where errors as large as ±50% are possible. Peak energies are good

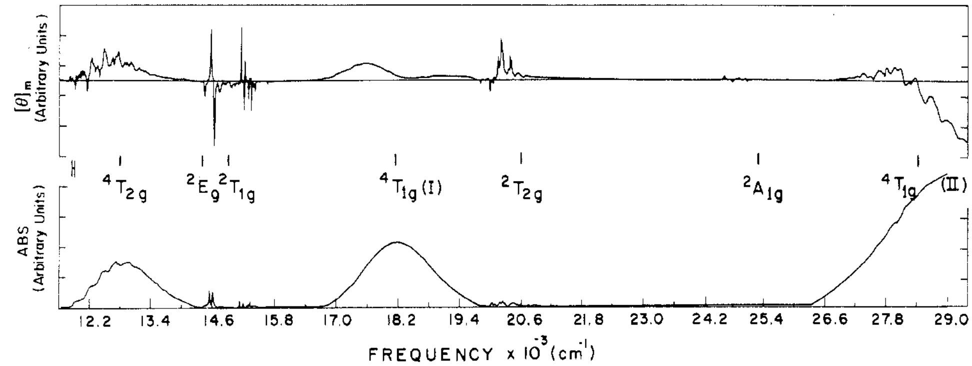

Figure 1. Visible absorption and MCD spectra of Cr^{3+}:Cs_2NaYCl_6 at 6 K. Also shown are the term energies calculated with the parameters given in the text. The maximum slit width is given at the left on the spectra. All spectra have been digitized by hand.

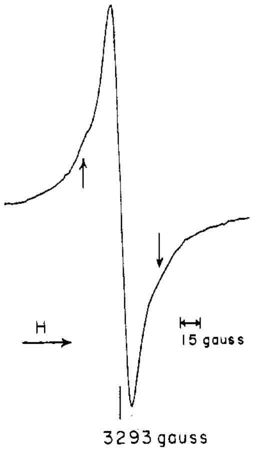

Figure 2. Room-temperature EPR spectrum of a single-crystal sample of Cr^{3+}:Cs_2NaYCl_6 taken at an arbitrary orientation. The arrows show shoulders possibly due to the two outermost nuclear hyperfine transitions. $\nu = 9144$ MHz.

to ±10 cm^{-1} with energy differences good to ±5 cm^{-1} for resolved transitions. In some cases large line widths and overlap in the spectrum will cause larger errors.

Results

The absorption and MCD spectra at ~6 K of Cr^{3+}:Cs_2NaYCl_6 for the entire region of interest are shown in Figure 1. The energy level diagram for this ion is well known and need not be repeated here. Also shown in Figure 1 are the calculated energies of the observed crystal field terms. Parameters used in this calculation are $F_2 = 1050$, $F_4 = 90$, $Dq = 1280$, and $\alpha = 78.2$, all in cm^{-1}. This calculation utilized computer programs written by Dr. J. A. Spencer of Southern Illinois University, Edwardsville, Ill., which diagonalize the combined matrices for the electrostatic and crystal field interactions as well as the Trees (α) correction. The spin-orbit coupling matrix was also included in these calculations, but because no single value of ζ satisfies all terms (vide infra), these results are not included at this point. With the exception of the $^2T_{2g}$ term at ~20 000 cm^{-1} the fit between the measured and calculated energies is satisfactory.

Ground-State Properties. EPR spectra were recorded at room temperature using both powders and a single-crystal sample. The single-crystal resonance is shown in Figure 2. The g value was found to be 1.984 ± 0.001 and no fine structure was observed. This indicates the zero-field splitting ($2D$) is very small. The site symmetry appears to be O_h as expected.[12] It has been shown[13] that Cs_2NaYCl_6 does *not* undergo the low-temperature crystalline phase change that occurs in some compounds with this composition and it is expected that the Cr^{3+} ion still has O_h symmetry at liquid helium temperature where the optical results were recorded. This is supported by the optical results themselves which show no splitting due to a lower symmetry crystal field component.

Also indicated in Figure 2 are some weak shoulders on the resonance which occur at about the right place (~32 G)[6] to be the two outermost nuclear hyperfine transitions due to the ^{53}Cr isotope with $I = {}^3/_2$ and an abundance of ~9.5%.

Another possibility is that strain effects have given rise to different local distortions at the Cr^{3+} sites.[7] This would cause a range of values for the zero-field splitting, $2D$. The spectrum would show an average over these sites and the observed shoulders would be the outermost transitions for the largest value of $2D$.[8] This would be ~32 G.

The ground state of Cr^{3+} in an O_h crystal field is $^4A_{2g}$. This term has no orbital angular momentum and to first order should give a g value equal to that of the free electron. In double-group notation this state is U′,[16] and second-order, and higher, spin-orbit coupling effects will addmix some U′ character from the excited $^4T_{2g}$ term. (This mixing is also responsible for all nonzero c_0 MCD.) The second-order correction to the g value[17] is

$$g = 2.0023 - 8\zeta/3\Delta \quad (\Delta = 10Dq)$$

Using the experimental g value and a range of Δ from 12 500 to 13 100 cm^{-1}, ζ_1, the one-electron spin-orbit coupling parameter, is found to be 88 ± 7 cm^{-1}. The results of the complete diagonalization give a value of 74 ± 6 cm^{-1}. This is somewhat lower and it appears that care must be exercised in using the results of the perturbation treatment.

$^2E_g(U') + {}^2T_{1g}(U' + E')$ Terms. Figure 3 shows the 6-K absorption and MCD spectra for transitions to these two terms. Energies, calculated and experimental c_0 values, and assignments for the various lines are reported in Tables I and II. The MCD results generally support the assignments given. Reasons for any major discrepancies are given below.

A normal-coordinate analysis of the molecule A_2BMX_6 has been carried out.[18] Of the ten vibrations found, five are of ungerade symmetry, four are t_{1u} and one is t_{2u}. In the compounds $Cs_2NaLnCl_6$ (Ln = Pr and Eu)[1c,d] the spectra show all of these ungerade vibrations along with transitions due to absorption of light at places other than the center of the Brillouin zone. In these systems the splittings between the longitudinal and transverse modes of some of the ungerade vibrations were also clearly resolved. In the present case the vibrational assignments are given primarily for the $CrCl_6^{3-}$ moiety. Some additional gerade vibrations are possibly observed in this spectrum, but all five of the ungerade vibrations seen in the lanthanide compounds are not seen. Also, there is no evidence in the Cr^{3+} spectrum for transitions due to $k \neq 0$ absorption nor a splitting of TO and LO modes of the t_{1u} vibrations.

In addition to the magnetic dipole allowed origin at 14 435 cm^{-1} the two major absorptions in the $^2E_g(U')$ term are the

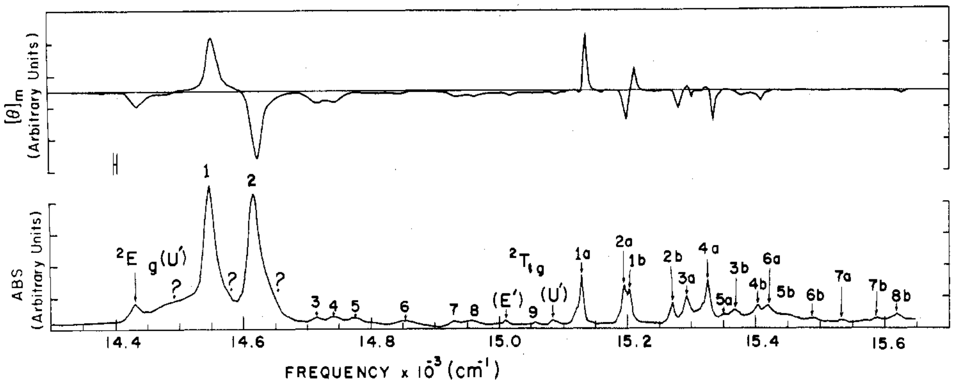

Figure 3. Absorption and MCD spectra of the $^4A_{2g}(U') \rightarrow {}^2E_g(U')$ and $^2T_{2g}(E' + U')$ transitions at 6 K. The origins and many of the vibrations are marked (see Tables I and II).

Table I. Analysis of the $^4A_{2g}(U') \rightarrow {}^2E_g(U')$ Transition in Cr^{3+}:Cs_2NaYCl_6 at 6 K

Line	Energy,[a] cm^{-1}	ΔE,[a,b] cm^{-1}	c_0 Exptl[c]	c_0 Calcd[d]	Assignment[e]
	14 430	0	−1.3	−1.25	0–0 $^2E_g(U')$
	14 480[e]	50	?[f]	−1.25	$+S_g$(lattice)?
1	14 548	118	+0.44	+0.63	$+S_{10}(t_{2u})$
2	14 617	187	−0.60	−0.63	$+S_6(t_{1u})$
	14 660	230	?	−1.25	$+S_2(e_g)$?
3	14 715	235	−1.5[g]	−1.25	$(+S_g$(lattice)$) + S_2(e_g)$
4	14 740	310	−1.3[g]	−1.25	$+S_1(a_{1g})$
5	14 775	227	(+)[h]	+0.63	$(+S_{10}(t_{2u})) + S_2(e_g)$
	14 800	320	(−)[h]	−1.25	$(+S_g$(lattice)$) + S_1(a_{1g})$
6	14 845	228	−0.43[i]	−0.63	$(+S_6(t_{1u})) + S_2(e_g)$
	14 860	312	(+)	+0.63	$(+S_{10}(t_{2u})) + S_1(a_{1g})$
	14 888	458	?	−1.25	$+2S_2(e_g)$?
7	14 928	311	−1.0[i]	−0.63	$(+S_6(t_{1u})) + S_2(a_{1g})$
	14 940	460	?	−1.25	$(+S_g$(lattice)$) + 2S_2(e_g)$
8	14 960	300	−0.85	−1.25	$(+S_2(e_g)) + S_2(a_{1g})$
	15 000	452	?	+0.63	$(+S_{10}(t_{2u})) + 2S_2(e_g)$
9	15 057	627	(−)	−1.25	$+2S_1(a_{1g})$
	15 070	453	(−)	−0.63	$(+S_6(t_{1u})) + 2S_2(e_g)$?

[a] Energy ±10 cm^{-1}; ΔE ±5 cm^{-1}. [b] ΔE from appropriate origin. [c] Error ±20% unless otherwise noted; measured using peak heights. [d] From Table VIII of ref 5. [e] Vibrations given in the notation of ref 18. [f] ? = not definitely observed. [g] Error ±33%. [h] MCD and/or *D* not resolved enough to determine quantitatively; sign of MCD measured. [i] Error ±50%.

Table II. Analysis of the $^4A_{2g}(U') \rightarrow {}^2T_{1g}(E' + U')$ Transition in Cr^{3+}:Cs_2NaYCl_6 at 6 K

Line	Energy,[a] cm^{-1}	ΔE,[a,b] cm^{-1}	c_0 Exptl[c]	c_0 Calcd[d]	Assignment[e]
	15 010	0	−0.90	−1.5	0–0 $^2T_{1g}(E')$
1a	15 130	120	+1.32	+1.05 ± 0.29	$+S_{10}(t_{2u})$
2a	15 196	186	−0.91	−1.05 ± 0.29	$+S_6(t_{1u})$
3a	15 293	233	$-c_0/+a_1$[f]	−1.5	$(+S_g$(lattice)$) + S_2(e_g)$
4a	15 326	316	$-0.91/+a_1$[f]	−1.5	$+S_1(a_{1g})$
5a	15 355	225	(+)[f]	+1.05 ± 0.29	$(+S_{10}(t_{2u})) + S_2(e_g)$
6a	15 420	224	(−)[f]	−1.05 ± 0.29	$(+S_6(t_{1u})) + S_2(e_g)$
7a	15 535	525	(−)	−1.5	$+S_2(e_g) + S_1(a_{1g})$
	15 083	73[g]	−0.61	−0.71	0–0 $^2T_{1g}(U')$
1b	15 203	120	+0.78	+0.64 ± 0.35	$+S_{10}(t_{2u})$
2b	15 271	188	−0.96	−0.64 ± 0.35	$+S_6(t_{1u})$
3b	15 370	237	(−)	−0.71	$(+S_g$(lattice)$) + S_2(e_g)$
4b	15 405	322	−0.66	−0.71	$+S_1(a_{1g})$
5b	15 425	222	?[h]	+0.64 ± 0.35	$(+S_{10}(t_{2u})) + S_2(e_g)$
6b	15 492	221	(−)	−0.64 ± 0.35	$(+S_6(t_{1u})) + S_2(e_g)$
7b	15 590	220	?	−0.71	$(+S_g$(lattice)$) + 2S_2(e_g)$
8b	15 620	537	−0.66	−0.71	$+S_2(e_g) + S_1(a_{1g})$

[a] Energy ±10 cm^{-1}; ΔE ±5 cm^{-1}. [b] ΔE from appropriate origin. [c] Error ±20%; measured using peak heights. [d] From Table VIII of ref 5. [e] Vibrations in notation of ref 18. [f] MCD and/or *D* not resolved enough to determine quantitatively; sign of MCD given. [g] ΔE from *E′* origin. [h] Not definitely observed.

t_{2u} vibration at 117.5 cm^{-1} and the $t_{1u}(1)$ vibration at 187 cm^{-1}. These energies are reasonable for metal–halide vibrations of this sort.[19] The different signs of the MCD clearly establish the different symmetries of the active vibrations. Two much weaker vibrational lines are seen at 284 and 310 cm^{-1} from the origin. On the basis of their energies and c_0 values they are assigned respectively as a combination band (Table I) and the a_{1g} vibration of the $CrCl_6^{3-}$ moiety. All vibrations also show a repeat in the a_{1g} mode and there are indications that a third member of this progression is also present (see Figure 3). In the combination bands the t_{2u} vibration shows up in the MCD as a minimum in an otherwise negative region. No additional t_{1u} vibrations are clearly observed although a second mode of this symmetry could be present very weakly at ~285 cm^{-1}. A large difference in intensities between the two t_{1u} vibrations has been noted in other systems[20] and indicates that in this case the lower energy vibration gives rise to a better electron–lattice coupling in this term. Beginning at 14 728 cm^{-1} the spectrum is again seen to repeat itself with an energy difference of ~230 cm^{-1} between the members of the progression. This energy is similar to what has been observed for e_g vibrations, and as the c_0's show no change in sign or magnitude (indicating activation by a gerade vibration), it is so assigned. The positive MCD for the t_{2u} line again shows up as a minimum in the otherwise negative MCD in this region. This type of progression involving an e_g vibration has been observed previously in $Cr(NH_3)_6^{3+}$.[8] A third member of this progression can be seen very weakly in absorption at ~15 000 cm^{-1} ($t_{2u} + 2e_g$) and ~15 085 cm^{-1} ($t_{1u}(1) + 2\,e_g$). The MCD associated with these absorptions, also extremely weak, shows the correct sign in each case, the t_{2u} line again

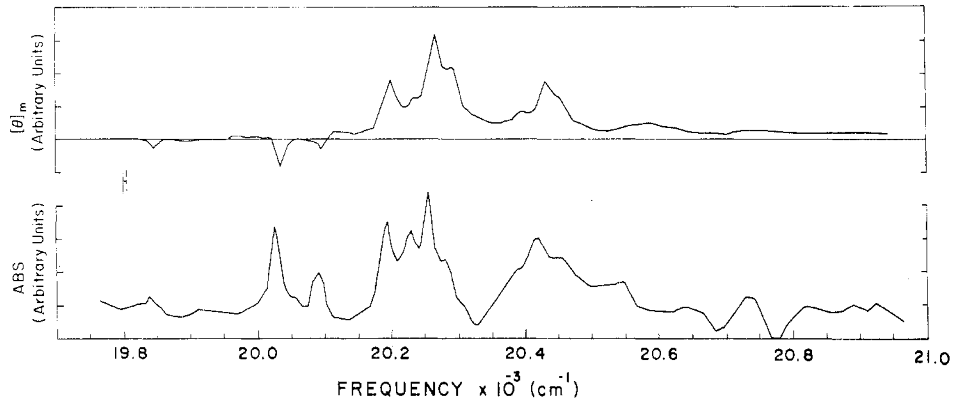

Figure 4. Absorption and MCD spectra of the $^4A_{2g}(U') \rightarrow {}^4T_{2g}(E'' + U')$ transitions at 6 K. For the absorption spectrum only a sharply increasing background has been subtracted. Note that this transition was recorded on a 0.1 OD scale.

corresponding to a minimum in an otherwise negative MCD.

Several other weak vibrational lines might also be present. The absorption spectrum shows evidence for one, or more, of these in the 25–100-cm^{-1} range above the origin. It is this vibration + e_g that is seen at 24 728 cm^{-1}. Evidence from the $^4T_{2g}$ term (vide infra) indicates a gerade vibration at ~115 cm^{-1}. Such a vibration, if present in the ^2E_g term, would explain the low c_0 measured for the line due to the t_{2u} vibration. Any gerade vibration will have an MCD of the same sign as the origin which is negative in this case. As this is opposite in sign to the MCD from the t_{2u} vibration, the MCD at this energy will be reduced while the absorption will be increased. Thus c_0, which is MCD/D, will decrease. Finally the line shape of the $t_{1u}(1)$ vibration in absorption shows an asymmetry to the high-energy side. This could be caused by an absorption in the 200–250-cm^{-1} region and might be the repeat of the origin in the e_g vibration.

The two magnetic dipole origins of the $^2T_{1g}$ term are observed at 15 009 (E′) and 15 083 cm^{-1} (U′). The relative magnitudes of c_0 for these lines[5] and the results of the "complete" crystal field calculations were used to determine the order of these two spin–orbit states. This calculation and the observed 74-cm^{-1} separation of these state gives a value of 230 cm^{-1} for the spin–orbit coupling constant ζ in this term. The vibronic assignments (see Table II) are essentially the same as in the ^2E_g transition. There are some small differences in energy for the various vibrations and a difference in relative intensities. This difference could indicate a difference in coupling strength to the lattice or a slightly different degree of distortion in the excited states.[21] The experimental c_0's are also given in Table II. Any discrepancies between the experimental and theoretical values are unexplained as of now.

Some a_1 character is also visible on some of the lines in this transition. This is due to the relative sharpness of these lines. The size of an a_1 term goes as the square of the line width and so any such character in the other lines could easily be too broad to see.

$^2T_{2g}(U' + E'')$ Term. The absorption and MCD spectra at 6 K for this term are shown in Figure 4. This region presents several difficulties in interpretation and at present very little can be said in the way of a detailed assignment. The first problem is the negative MCD of the lowest energy lines. A magnetic dipole origin for E″ and any t_{1u} or gerade vibrations built on that origin must have a positive MCD.[5] This is because all allowedness evolves from mixing some E″ character from a $^4T_2$ term, and as has been shown[5] this spin–orbit component has a positive MCD. The same is true for U′ in that, to first order in perturbation theory, only the $U'_{3/2}$ component of $^4T_{2g}$ can mix with this term and this component also has a positive MCD in its origin and t_{1u} and gerade vibrations.[5] $U'_{5/2}$ could possibly mix in a higher order approximation and this component has a negative MCD. However this mixing should be very small and the MCD should still be dominated by the $U'_{3/2}$. Cross terms between the two U′ terms should also be small and not greatly affect the sign of the MCD.

One possible source of negative MCD in both of these spin–orbit states is coupling to a t_{2u} vibration. This however is not the solution. First of all there can only be two t_{2u} vibrations and at least three negative terms are observed. Also unless vibrational energies are drastically different, an unexpected effect, each t_{2u} vibration (negative MCD) should have a t_{1u} vibration (positive MCD) about 70 cm^{-1} higher in energy as well as a magnetic dipole origin (positive, MCD) about 117 cm^{-1} lower in energy. Neither of these is observed. Another possibility for this negative MCD is its being due to a Cr^{3+}–Cr^{3+} pair. A variation in concentration showed no change in relative intensities between these lines and the rest of the spectrum so that too is elminated. This problem has been observed previously but not commented on. In particular Figures 1 and 3 of ref 5 show a minimum in an otherwise positive MCD that is quite obviously caused by a transition at that energy having a negative MCD.

Even ignoring the negative MCD this transition presents difficulties in interpretation. No obvious origins are present and no vibrational patterns similar to those in the ^2Eg, $^2T_{1g}$, or $^4T_{2g}$ (vide infra) terms can be seen. The absence of origins is understandable as they are expected to be very weak.[5] One interesting feature is the apparent progression beginning at ~20 250 cm^{-1} and showing four members (six in a more concentrated sample), each member being composed of three or four components. This is reminescent of the $^2T_{2g}$ transition in Cr^{3+}:alum.[5] In that case the separation was ~300 cm^{-1} and was assigned as a progression in a_{1g} built on a t_{1u} false origin. An additional splitting of 50–80 cm^{-1} was assigned as the separation of the two spin–orbit components.

In the present case the separation between members of the progression would be 165–195 cm^{-1}. This is much too small to be the a_{1g} mode although it is at the correct energy to be a t_{2g} vibration.[19] Another possibility is that this region is showing two different progressions originating on the two spin–orbit components of $^2T_{2g}$. This however would require a value of ζ between 275 and 325 cm^{-1} to account for the splitting and leave an energy of 330–390 cm^{-1} for the activating vibration. Neither of these latter two conditions seems probable. It is possible that the spectrum is caused by a dynamic Jahn–Teller effect,[9] but a solution of this type of problem is beyond the scope of the present publication.

$^2A_{1g}(E')$, Pair Spectra (?), and Higher Energy Doublets. The energy region about 24 800 cm^{-1} shows four to six extremely weak lines in the MCD spectrum (Figure 1). Neither undoped Cs_2NaYCl_6 nor Cs_2NaYCl_6 doped with Fe^{3+}, Co^{2+},

Table III. MCD of the $^4A_{2g}(U') \rightarrow {}^4T_{2g}$ Transitions in Cr^{3+}:Cs_2NaYCl_6 at 6 K[g]

Term origins	Energy,[a] cm^{-1}	ΔE, cm^{-1}		Rel MCD	
		Calcd[b]	Exptl[c,d]	Calcd[e]	Exptl[f]
E″	11 809			+1.25	+2.00
$U'_{3/2}$	11 845	33	36	+1.00	+1.00
$U'_{5/2}$	11 892	43	47	−1.50	−1.00
E′	11 908	20	16	−0.75	−4.00

[a] Error ±10 cm^{-1}. [b] Using the "complete" crystal field calculation with $\zeta = 150$ cm^{-1} and other parameters as given in the text. [c] Error ±5 cm^{-1}. [d] Measured from preceding line. [e] Tables II and III of ref 5. [f] Error ±50%; measured as relative heights only. [g] The stick spectrum in Figure 5 was generated using $S_g = 115$ cm^{-1}, $S_{10}(t_{2u}) = 130$ cm^{-1}, $S_6(t_{1u}) = 195$ cm^{-1}, $S_2(e_g) = 240$ cm^{-1}, and $S_1(a_{1g}) = 300$ cm^{-1}.

or Ni^{2+} shows any MCD in this region. The relative intensity of these lines compared to that of the rest of the spectrum does not increase in a more heavily concentrated sample. It is thus concluded that they are due to transitions in the Cr^{3+} ion. The $^2A_{1g}(E')$ term is expected to fall at about this energy (Figure 1) and these lines are tentatively assigned as being transitions to that term. No origin is expected for this transition and the signs of the MCD[5] and the energy separation of the first three lines are consistent with their being a t_{2u} vibration and two t_{1u} vibrations, respectively. This three-line pattern is then repeated with an interval of about 300 cm^{-1}, the correct range for the a_{1g} vibration.

In the less concentrated sample these lines are superimposed on a barely discernible broad positive MCD. In the more concentrated sample this MCD is increased dramatically in relative intensity. The peak of this broad MCD is at about 24 600 cm^{-1}. This is roughly twice the energy of the $^4T_{2g}$ term. Doubly excited pair spectra have been observed[22] at about twice the energy of the equivalent single ion transition and Cr^{3+}–Cr^{3+} pairs could be the cause of this broad MCD. Further work on Cr^{3+}–Cr^{3+} interactions in this material is planned.

The crystal field calculation predicts four transitions to doublet terms between 27 375 and 27 530 cm^{-1}. As Figure 1 shows there is a good deal of fine structure in the MCD in this energy region superimposed on the broader, more intense absorption that probably belongs to the $^4T_{1g}(II)$ term (vide infra). No detailed assignments have been made in this region of the spectrum. At energies just above those shown in Figure 1 the intense charge-transfer bands begin and no further d–d spectra can be recorded.

$^4T_{2g}$ Term. The MCD for this transition is shown in Figure 5. Also shown are the calculated positions and relative MCD values of all lines assuming the same vibrational analysis as for the ^2E_g and $^2T_{1g}$ terms and the vibrational energies given in Table III. No account is taken of Franck–Condon factors. For the most part the signs calculated[5] for the MCD agree with those observed, particularly in the early part of the spectrum, below 12 200 cm^{-1}, where any other effects should be their smallest. The overall positive nature of the MCD in this term and the other quartets is due to the mixing of some $U'(^4T_{2g})$ character into the ground state. This effect has not been accounted for in the calculations of the MCD of transitions to individual spin–orbit components. The absorption spectrum in this region shows none of the detail observed in the MCD (Figure 1). This phenomenon has been observed previously in many other systems.[4,5]

In an O_h crystal field the $^4T_{2g}$ term is split by spin–orbit coupling into four levels. The "complete" crystal field calculation gives their energies as $E'' < U'_{3/2} < U'_{5/2} < E'$, the highest two levels being split only by second-order, and higher, effects.[16] The first three absorptions are assigned as the four magnetic dipole allowed no-phonon transitions. The third line is actually a composite of the $U'_{5/2}$ and E′ terms, their separation (~20 cm^{-1}) not being great enough to allow them to be resolved. Vibrational assignments here are essentially the same as in the doublets. The energies of most vibrations are slightly larger but the same progressions in e_g and a_{1g} vibrations are clearly observed. The e_g progression is most easily seen for the $U'_{5/2}$ + E′ line. The origin for these two terms appears as a negative MCD at ~11 908 cm^{-1}. A repeat of this line is seen, also with a negative MCD, at ~12 145 cm^{-1}, the difference being 237 cm^{-1}. The second member of the progression is seen ~235 cm^{-1} higher in energy at ~12 380 cm^{-1}. In this case it is observed as a minimum in an otherwise positive MCD as are a number of other vibrations. The other terms are not as obvious, due to overlapping transitions, but still can be seen. Figure 5 shows, for each spin–orbit component, a 0–0 line, a gerade vibration, and the $S_{10}(t_{2u})$ and $S_6(t_{1u})$ modes. There is also shown a repeat of each of these in $S_2(e_g)$, $S_1(a_{1g})$, $2S_2(e_g)$, $S_1(a_{1g})$ + $S_2(e_g)$, $2S_1(a_{1g})$, $3S_2(e_g)$, and $2S_2(e_g) + S_1(a_{1g})$. Note in the figure how as the energy increases and more lines are expected, the observed spectrum broadens into being practically featureless, due to the severe amount of overlap.

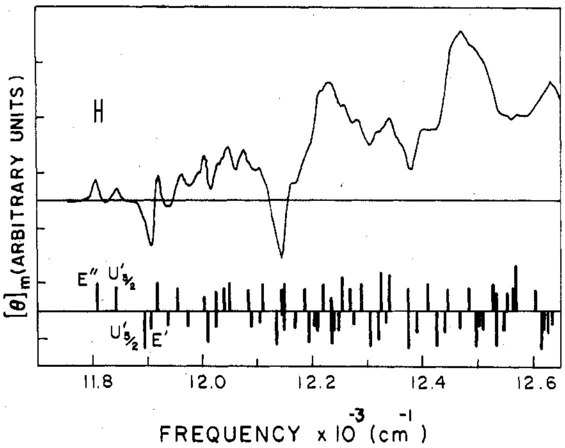

Figure 5. MCD spectrum for the $^4A_{2g} \rightarrow {}^4T_{2g}$ transitions at 6 K. The four origins are shown. The stick spectrum was generated using the vibrational energies given in Table III. Relative intensities were calculated using Tables II and III of ref 5. No account has been taken of Franck–Condon factors or ground-state mixing.

The temperature dependence of the absorption intensity was measured at 6, 77, and 300 K. Using the hyperbolic cotangent law[23] an energy of ~150 ± 30 cm^{-1} was found for the activating vibration. This is in only fair agreement with the ~195 cm^{-1} found for the $t_{1u}(1)$ vibration.

Absorption by this term in VF_6^{4-} showed a pronounced quenching of the spin–orbit splitting in the first vibronic term.[9] In the present case the observed spectrum can be assigned using a value of $\zeta \approx 150$ cm^{-1}. This decrease from the free-ion value of 270 cm^{-1} [7] is more indicative of covalency than a Ham effect[24] and so this latter effect was not considered here.

$^4T_{1g}$(I and II) Terms. The absorption to the $^4T_{1g}(I)$ term shows a maximum at ~18 200 cm^{-1} (Figure 1). The MCD clearly shows a positive maximum at ~17 600 cm^{-1}, a minimum (negative MCD superimposed on a larger positive MCD) at ~18 500 cm^{-1}, and an additional weaker positive MCD at ~19 100 cm^{-1}. This pattern, similar to that observed in $Cr(H_2O)_6^{3+}$,[5] is readily explained by the results of a crystal field calculation and the MCD calculations given in Table II of ref 5. The crystal field calculations show the lowest two spin–orbit components are separated by only 10–25 cm^{-1}. The lowest level is the E″ which should show a negative MCD. The next level, $U'_{5/2}$, shows a more intense positive MCD which will dominate the spectrum in this region. At somewhat higher energies, 50–90 cm^{-1} above $U'_{5/2}$, the $U'_{3/2}$ with its negative MCD is observed. The final term, E′, shows a positive MCD and this is seen as the final, much weaker, positive peak.

The absorption spectrum at 6 K shows no vibrational structure. The MCD does show some indications of structure but in general it is too broad to be assigned. The temperature dependence of the absorption was measured and the energy of the activating vibration found to be 325 ± 65 cm^{-1}. This indicates that for this term the higher energy t_{1u} vibration may be the activating mode. Activation of the $^4T_{1g}$ and $^4T_{2g}$ transitions by different vibrations has been observed in other Cr^{3+} systems.[25] The difference in resolution of vibronic lines has also been seen.[4,5]

The $^4T_{1g}$(II) level is observed at ~28 400 cm^{-1} as a shoulder on an extremely intense (charge-transfer?) transition (Figure 1). This is the expected energy based on the crystal field calculation. Very little structure is seen in the absorption. The MCD shows some additional structure, but because of the possibility of there being some doublets absorbing at the same energies and the overlap with the intense band, nothing quantitative can be said at this time.

Discussion

The value of 10*Dq* found in the present study is 820 cm^{-1} smaller than that in $CrCl_3$[7] and appears to be the smallest yet reported. This could be strictly a crystal field effect. In the present case the chlorides will be much further away from the Cr^{3+} than in $CrCl_3$. The Y–Cl distance in Cs_2NaYCl_6 is ~2.68 Å[12] while the Cr–Cl distance in $CrCl_3$ is only 2.34–2.37 Å.[24] The Cr–Cl distance in Cs_2NaYCl_6 will be somewhat smaller than the Y–Cl distance, but it is likely to be larger than the distance in $CrCl_3$.[27]

A more interesting point to note is the large variation in ζ with how it is determined. The value found for the ground state from the EPR g value is ~74 cm^{-1}. The value found in the $^4T_{2g}$ term is ~150 cm^{-1} while that in the $^2T_{1g}$ term is ~230 cm^{-1}. The actual number determined in all of these measurements is $k\zeta$ where k is the orbital reduction factor, a measure of covalent bonding.[26] If the entire change in $k\zeta$ is ascribed to changes in k, then values of k for the three terms are $k(^4A_{2g}) = 0.27$, $k(^4T_{2g}) = 0.56$, and $k(^2T_{1g}) = 0.85$, where covalency *increases* as *k decreases*. While the numerical values of k given above may not have any great significance, their relative values probably do. Thus there is an obvious trend toward a larger quenching of the orbital angular momentum with *decreasing* energy of the terms with $k(^2T_{1g}) \approx 3k(^4A_{2g})$ and $k(^4T_{2g}) \approx 2k(^4A_{2g})$. This is the opposite direction expected if this quenching were due to mixing with excited terms. For an explanation of this trend one must go back to the strong-field configurations giving rise to these terms and consider their character.

The t_{2g} orbitals on Cr^{3+} are, to a first approximation, nonbonding. They will, however, overlap with π orbitals on the chlorides thus gaining some bonding character. The e_g metal orbitals are strictly σ antibonding. Thus a term arising from a strong-field configuration involving primarily t_{2g} orbitals should show the effects of bonding more than one with some e_g character. The major effect of bonding will be to delocalize the electrons and cause a reduction in factors such as ζ.

The $^4A_{2g}$ term in Cr^{3+} arises strictly from the t_{2g}^3 configuration.[17] The $^4T_{2g}$ term comes only from the $t_{2g}^2e_g$ configuration while the $^2T_{1g}$ term contains t_{2g}^3, $t_{2g}^2e_g$, and $t_{2g}e_g^2$. Thus the term with the most t_{2g} character, i.e., most ligand-bonding character, shows the largest reduction in ζ while that with the most e_g character shows the smallest reduction. Additional support for this interpretation is found by comparing the vibrational energies in the $^4T_{2g}$ and $^2T_{1g}$ terms. Both the $t_{1u}(1)$ and the t_{2u} vibrational energies are larger in the $^4T_{2g}$ term than in the $^2T_{1g}$ term, while the e_g vibrational energy is practically unchanged. Observing the deformations caused by these vibrations[19] shows both t_u vibrations will affect the t_{2g} orbitals while the e_g vibration will not. Thus the term with the larger reduction in ζ, the $^4T_{2g}$, also shows the higher vibrational energies, both effects being indicative of increased bonding.

Acknowledgment. The author thanks Dr. Paul. N. Schatz for the use of his equipment and his constant encouragement. A Cottrell grant from the Research Corp. to the author made possible the purchase of the Spectro-Mag II.

Registry No. Cr^{3+}, 16065-83-1; Cs_2NaYCl_6, 27880-16-6.

References and Notes

(1) (a) R. W. Schwartz and P. N. Schatz, *Phys. Rev. B*, **8**, 3229 (1973); (b) R. W Schwartz and N. J. Hill, *J. Chem. Soc., Faraday Trans. 2*, **70**, 124 (1974); (c) R. W. Schwartz, *Mol. Phys.*, **30**, 81 (1975); (d) R. W. Schwartz, *Mol. Phys.*, in press.
(2) J. Ferguson, H. J. Guggenheim, and D. L. Wood, *J. Chem. Phys.*, **54**, 504 (1971).
(3) See, for example, P. J. Stephens, *Annu. Rev. Phys. Chem.*, **25**, 201 (1974), and references therein.
(4) K. Y. Wong, D. Sengupta, and D. J. Mackey, *J. Phys. Chem. Solids*, **35**, 313 (1974).
(5) M. J. Harding and B. Briat, *Mol. Phys.*, **27**, 1153 (1974).
(6) B. R. McGarvey, *Transition Met. Chem.*, **3**, 89 (1966), and references therein.
(7) H. Witzke, *Theor. Chim. Acta*, **20**, 171 (1971), and references therein.
(8) C. D. Flint and P. Greenough, *J. Chem. Soc., Faraday Trans. 2*, **68**, 897 (1972).
(9) M. D. Sturge, *Phys. Rev. B*, **1**, 1005 (1970).
(10) F. S. Ham, *Phys. Rev A*, **138**, 1727 (1965).
(11) The notation used here is that of ref 5.
(12) L. R. Morss, M. Siegal, L. Stenger, and M. Edelstein, *Inorg. Chem.*, **8** 1433 (1969).
(13) R. W. Schwartz, S. F. Watkins, C. J. O'Connor, and R. L. Carlin, *J. Chem. Soc., Faraday Trans. 2*, **72**, 565 (1976).
(14) B. R. McGarvey, *J. Chem. Phys.*, **37**, 3020 (1963).
(15) J. Brickmann and G. Kothe, *J. Chem. Phys.*, **59**, 2807 (1973).
(16) J. S. Griffith, "The Theory of Transition-Metal Ions", Cambridge University Press, New York, N.Y., 1961.
(17) J. W. Orton, "Electron Paramagnetic Resonance", ILIFFE Books Ltd., London, 1968.
(18) A. Z. Lentz, *J. Phys. Chem. Solids*, **35**, 827 (1974).
(19) J. R. Ferraro, "Low-Frequency Vibrations of Inorganic and Coordination Compounds", Plenum Press, New York, N.Y., 1971.
(20) S. B. Piepho, J. R. Dickinson, J. A. Spencer, and P. N. Schatz, *J. Chem. Phys.*, **57**, 982 (1972).
(21) C. D. Flint and P. Greenough, *J. Chem. Soc., Faraday Trans. 2*, **70**, 815 (1974).
(22) J. J. Krebs and W. G. Maisch, *Phys. Rev. B*, **4**, 757 (1971); J. P. van der Ziel, *ibid.*, **4**, 2888 (1971).
(23) A. J. McCaffery, J. R. Dickinson, and P. N. Schatz, *Inorg. Chem.*, **9**, 1563 (1970).
(24) W. C. Yeakel and P. N. Schatz, *J. Chem. Phys.*, **61**, 441 (1974).
(25) R. L. Carlin and I. M. Walker, *J. Chem. Phys.*, **46**, 3921 (1967).
(26) B. Morosin and A. Narath, *J. Chem. Phys.*, **40**, 1958 (1964).
(27) W. R. Hurren, H. M. Nelson, E. G. Larson, and J. H. Gardner, *Phys. Rev.*, **185**, 624 (1969).
(28) K. W. H. Stevens, *Proc. R. Soc. London, Ser. A*, **219**, 542 (1953).